



MALAYSIAN JOURNAL OF BIOCHEMISTRY AND MOLECULAR BIOLOGY

The Official Publication of The Malaysian Society For Biochemistry and Molecular Biology (MSBMB)

<http://mjbmb.org>

PHARMACOPHORE-BASED MOLECULAR DOCKING AND *IN-SILICO* STUDY OF NOVEL USNIC ACID DERIVATIVES AS AVIAN INFLUENZA A (H7N9) INHIBITOR

Miah Roney^{1,2}, Kelvin Wong Khai Voon^{1,2}, AKM Moyeenul Huq², Kamal Rullah³, Saiful Nizam Tajuddin², Hazrulrizawati Abd Hamid¹, Mohd Fadhilzil Fasihi Mohd Aluwi^{1,2*}

¹*Faculty of Industrial Sciences and Technology, Universiti Malaysia Pahang, Lebuhraya Tun Razak, 26300 Gambang, Kuantan, Pahang Darul Makmur, Malaysia.*

²*Centre for Bio-aromatic Research, Universiti Malaysia Pahang, Lebuhraya Tun Razak, 26300 Gambang, Kuantan, Pahang Darul Makmur, Malaysia.*

³*Kulliyyah of Pharmacy, International Islamic University Malaysia (IIUM), Jalan Sultan Ahmad Shah, 25200 Kuantan, Pahang, Malaysia.*

*Corresponding Author: fasihi@ump.edu.my

History

Received: 30 April 2022

Accepted: 15 November 2022

Keywords:

Usnic acid; Pharmacophore; Molecular docking; Avian Influenza A

Abstract

The Avian Influenza virus is not only dangerous to birds, but it is also dangerous to people and other animals. It is a serious danger to poultry worldwide with the capacity to spread to other species, including people; consequently, more efficient medicines are required to treat this virus. This study examined the binding effectiveness of twenty-one (21) Usnic acid derivatives out of 340 generated *via* pharmacophore filtering with AIV A (H7N9) utilising an *in-silico* technique. The docking simulation to AIV A obtained five compounds with a high affinity to the target protein. The ADMET and druggability prediction produced two lead molecules that were then submitted to Cytochrome (CYP) P450 enzyme screening to generate the best molecule, labelled as compound 5. According to the findings, compound 5 might be employed as a lead inhibitor in developing an anti-AIV medication.

INTRODUCTION

Avian Influenza A (AIV) viruses are members of the *Orthomyxoviridae* family, which includes viruses that infect humans, birds, and a variety of animal species [1]. AIV, commonly known as bird flu, is a virus that may infect not just birds but also humans and other animals [2,3]. The AIV viruses H5, H7, and H9, which are common in domestic poultry, can infect people and cause moderate to deadly illnesses [1]. This virus has now become a serious public health concern throughout the world [4], and it is classified as Highly Pathogenic Avian Influenza (HPAI), resulting in numerous human and bird deaths [5].

AIV that is only circulating in avian species seldom infects people, whereas AIV that is only circulating in humans rarely transfers to avian species [6]. H5N1 AIV, a highly virulent AIV that arose in Hong Kong in 1996-97, had caused outbreaks in poultry or wild birds in over sixty

countries and 317 human cases, including 191 fatalities, by June 2007 [7]. South-East and East Asia were the first to be hit. Between the end of 2003 and the beginning of 2004, nine Asian countries, including China (confirmed 25 with 16 deaths), Turkey (confirmed 12 with 4 deaths), Azerbaijan (confirmed 8 with 5 deaths), Laos (confirmed 2 with 2 deaths), Thailand (confirmed 24 with 17 deaths), Cambodia (confirmed 7 with 7 deaths), Vietnam (confirmed 95 with 42 deaths), Iraq (confirmed 3 with 2 deaths) and Indonesia (confirmed 101 with 80 deaths) [8], announced human Avian Flu illnesses. H5N1 human infection had been discovered in 16 countries since December 14, 2015, with 499 of 844 cases dying [9]. In February 2013, it was announced that another AIV virus, H7N9, infected humans in China [6]. Other Asian countries, such as Taiwan, Hong Kong, and Malaysia, have also been affected. Six hundred eighty-four humans affected by H7N9 AIV had been documented as of December 26, 2015 [10], with at least 275 of those dying. More than 50

occurrences involving the AIV subtypes H5N1, H5N2, H5N3, H5N6, H5N8, H5N9, H7N3, and H7N9 were reported in 2015 from 33 countries [6].

AIV is not only pathogenic to birds, but certain avian viruses are also extremely pathogenic to humans and other animals. There have been three drugs (RWJ-270201, Oseltamivir and Zanamivir) developed against neuraminidase (NA) enzyme of Influenza A and Influenza B but need the annual updating because these drugs are ineffective against new subtype of AIV such as 2006-H5N1 [11,12]. Despite vaccines for AIV prophylaxis have been established, the increasing resistance strains severely restrict the efficacy of these principal preventive medications. As a result, innovative anti-AIV medications are being explored to combat the spread of this resistance dilemma. Natural products and their derivatives, which have a wide range of biological diversity, represent an unlimited resource for the creation of innovative anti-AIV medications.

AIV A virus is a lipid-enveloped virus with a negative-sense RNA genome that has eight segments. It is thought that a balance between the activities of the two surface glycoproteins hemagglutinin (HA) and neuraminidase (NA) is essential for viral reproduction and propagation [13]. Hemagglutinin protein subtypes (H1-H16) and neuraminidase protein subtypes (N1-N9) have been found so far [14,15]. The neuraminidase cleaves the specific connection of the sialic acid receptor, allowing freshly formed virions to be released from infected cells. Furthermore, in lung epithelial cells, the neuraminidase enzyme may help in the early phases of influenza virus infection [16].

Usnic acid is the most common secondary metabolites in lichens which has been shown to have various biological effects, including anti-viral activity [17,18]. In this study, 340 UA derivatives were investigated in pharmacophore filtering and the best fitted compounds were classified the binding interactions against the human affecting AIV A (H7N9) using molecular docking strategy based on anti-viral properties.

MATERIALS AND METHODS

Protein and Ligand Preparation

The crystallized structures of target protein (PDB ID: 4MWW; Resolution: 1.90) [19] was obtained from the Protein Data Bank (<https://www.rcsb.org/>) and used to create the protein with Discovery Studio 3.1. To seal the active sites, hydrogen atoms, missing amino acid residues, and loop segments were introduced before confirming that the different bond orderings were formed correctly. In addition, all crystallographic waters were eliminated from

the PDB file. Finally, the produced protein was saved in the .pdbqt file format.

340 Usnic acid derivatives (Supplementary Table S1) were employed that were gathered from the literature based on their anti-viral efficacy. Furthermore, the structures of the compounds were developed using the ChemDraw professional 14 programme. The preparation techniques were carried out using the default protocol defined in the Discovery Studio 3.1 programme to improve the structures of the ligands, correct the partial charge, reduce the molecular energy, and add missing hydrogen atoms under the CHARMM force field. Finally, all of the produced ligands were stored in the .sdf file format.

Pharmacophore Model Generation

HipHop pharmacophore characteristics were created by combining four active compounds against Avian Influenza A from four proteins (PDB IDs: 4MWV, 4MWW, 4MWX, and 4MWY) (Table 1). For all ligand, the most active compound in the training set was assigned a primary value of 2 and a maximal omit feature value of 0, whereas the remaining compounds were allocated 1 and 0 to designate them as moderately active [20]. Before developing the HipHop pharmacophore model, the pharmacophore module "Feature Mapping" was used to classify the important chemical properties of the training set of compounds. Using the molecular mechanics CHARMM force field, a training set was created in Catalyst's 2D/3D Visualizer and reduced to the nearest local minimum. The following building elements were used for the pharmacophore model: HBA (hydrogen bond acceptor), HBD (hydrogen bond donor), HC (hydrophobic feature), HAL (hydrophobic aliphatic), HAR (hydrophobic aromatic), PI (positive ionizable), and AR (aromatic ring). The "BEST" option was used to set to 255 conformations within a 20 kcal/mol energy barrier in order to get a broad variety of conformations. Table 2 lists and ranks the generated pharmacophore models that have substantial chemical similarities.

The techniques of Liu et al., (2020) were used in this investigation with minor modifications. In Liu et al., 2020 study, generated the HipHop Hypo from six active compounds with a target protein [21]. But in this study, we used four active compounds from four proteins to generate HipHop pharmacophore model. The four crystal structures of Avian-origin human-infecting H7N9 influenza viruses (PDB IDs: 4MWV, 4MWW, 4MWX, and 4MWY) [14] were selected to create the pharmacophore features from four co-crystallized compounds (Index Number 01 from 4MWV, Index Number 02 from 4MWW, Index Number 03 from 4MWX, and Index Number 4 from 4MWY) (Table 1). Figure 1 illustrated the workflow.

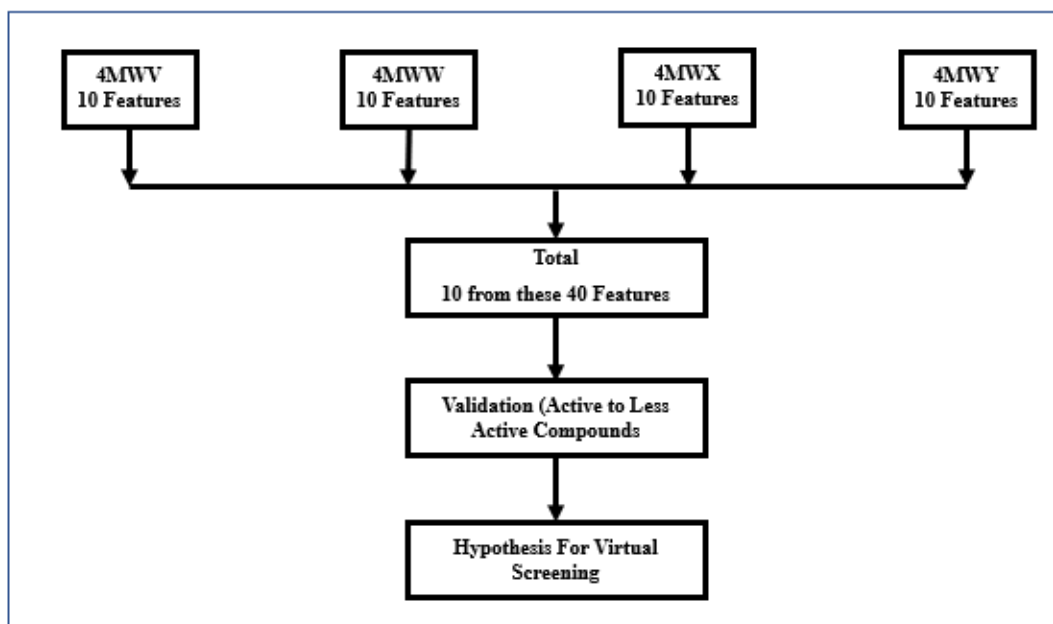


Figure 1. Avian Influenza A Virus pharmacophore model generation, validation, and virtual screening process

Validating The Pharmacophore Model

The fit results obtained using test sets support the pharmacophore concept. The test sets (Figure 2), which contained compounds with activity ranging from active to inactive [22], were created using the same manner as the training set. The notion was then put to the test with the "Ligand Profiler Module" to see if it could categorise the active chemicals based on the Fit Value.

Pharmacophore-based Virtual Screening

The HipHop-Hypo06 pharmacophoric model, which has been verified, was used to screen medicines. The literature search generated 340 usnic acid derivatives, which were subsequently put to virtual screening. All of those compounds were loaded into Discovery Studio 3.1, and the HipHop-Hypo06 compounds were screened using the DS3.1 "Screen Library" module. The conformation method was set to BEST with 255 conformations. The remaining parameters were left at their default defaults. Lastly, the chosen pharmacophore hypothesis was associated with specific chemical compounds associated with the Structural Activity Relationship (SAR) [23].

Molecular Docking

Molecular docking study was performed using Discovery Studio 3.1 [24] software. The selected ligands from pharmacophore filtering were individually docked against the protein targets (PDB ID: 4MWW) [19] to assess the ligand and receptor interactions under the CHARMM force

field. The best binding site was determined based on the co-crystallized ligand binding site, and the grid box was set at $-17.34 \text{ \AA} \times 26.48 \text{ \AA} \times 83.20 \text{ \AA}$ in size, with docking calculations performed inside a sphere with a radius of 10.73 \AA [25]. The binding location of the co-crystallized ligand, which was used as a reference medication due to its frequent use as an antiviral medicine that has been studied for AIV A, was used to determine the centre of the site sphere. All other parameters were left at their default values. The Top Hits parameter was set to 10, suggesting that the top ten conformations of each ligand were retained based on scoring and ranking by CDOCKER capacity. The selected Usnic acid derivatives were docked into the active region of target protein and were ranked based on the calculated binding energy of the ligand-target protein complex. The compounds with greater (more negative) binding energies than that of the co-crystallized ligand, when in complex with the receptor, were selected as the top hits. Finally, the molecular interactions were evaluated during the docking simulation. The binding energy was calculated in kcal/mol, with a lower value suggesting stronger ligand-target interactions. Utilizing Discovery Studio 3.1, we observed amino acids at the ligand-protein binding site using the 2D and 3D interaction forms of docked complex.

Molecular Docking Validation

The co-crystallized ligand was redocked into the target protein's binding areas using Discovery Studio 3.1 to validate and protein residue recognition. To investigate if docking was more predictable in the long run, we connected the observed contact energy and co-crystallized ligand. By

computing the ideal docked complex of the co-crystallized ligand and experimental compounds, the precision and efficiency of DS3.1 were proven.

ADMET Prediction

The ADMET profile may be used to evaluate a product's potential and safety prior to its release to the market by analysing absorption, dispersion, metabolism, excretion, and toxicity. Unwanted property compounds often increase patient expenditures and stress [26]. As a result, anticipating ADMET characteristics is crucial for hit detection and optimization. The ADMET characteristics of the examined drugs were evaluated using Discovery Studio 3.1. Initially, the Chemistry at CHARMM force field was used, and then the compounds were produced and minimised according to the Small Molecule Preparation Protocol. Then, using the "Small Molecules" tag, the ADMET descriptors procedure was used to carry out these experiments [27,28].

Drug-likeness Properties

The online server Molinspiration Cheminformatics (<http://www.molinspiration.com>) was used to analyse the bioactivity data of selected compounds [29]. Only structures for SMILES or SD-files are required for the production of active molecules; no knowledge in the active site or binding mode is necessary. This is especially beneficial when a framework approach is not viable due to unclear 3D receptor structure.

Analysis of CYP Isoform

The online server SwissADME (<http://www.swissadme.ch/>) software was utilised in the context of additional factors affecting drug metabolism in the body [30]. Cytochrome (CYP) P450, a specific CYP inhibitor, has been attempted. This predictor is an isozyme from the drug biotransformation family. CYP metabolism is required for the formation of a number of pharmacological activities in the body that result in toxic, pharmacokinetics, and undesirable drug responses.

RESULTS AND DISCUSSION

Pharmacophore Model Generation

The HipHop pharmacophore model was built utilising ten features based on each protein's rank value. Two characteristics from 4MWY, three from 4MWV, three from 4MWW, and two from 4MWX (from the same rank value, we chose the top one) were chosen based on the highest rank value.

According to the pharmacophore features, the top ten pharmacophore hypotheses with three characteristics were grouped into three groups: DDDAAA (01, 02), HHDDAA (03, 04, 05, 06, 07, 08), and DAAAA (09, 10). The

hypotheses in these four categories were determined by the position of features, the direction of hydrogen bond vectors, or both (Table 2).

Pharmacophore Validation

The most applicable pharmacophore model was chosen from 10 pharmacophore hypotheses created using the approach described by Liu et al., (2020) [21]. To create a test set, active to less active [10] AIV inhibitors were chosen from diverse sources (Figure 3). The chemicals in the test set corresponded to each of the 10 hypotheses, and the findings were presented on a Heatmap (Figure 3C). According to the Heatmaps, HipHop hypothesis 06 (HHHAA) was the most suited of the 10 pharmacophore hypotheses (Figure 3B). Figure 3A shows that a1, a2, and a3 were associated with the hydroxyl (-OH) group, the amine (-NH=) group, and the methyl (-CH₃) group, respectively. The methyl (-CH₃) group was also used to define the b1 and b2 characteristics, while the carboxyl (C=O) group was used to create the c1.

Pharmacophore-based Virtual Screening

The in-house database of 340 Usnic Acid derivatives was submitted to pharmacophore filtering using the previously generated HipHop Hypo06 pharmacophore model. Twenty-one (21) compounds were selected for further screening using the molecular docking procedure depending on the fit value of >3.3. (Supplemental Table S2)

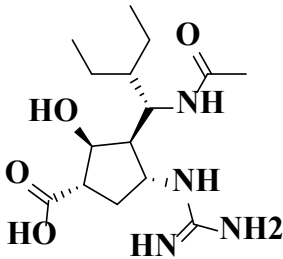
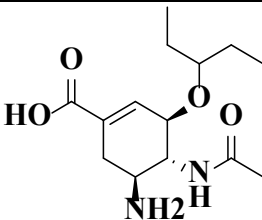
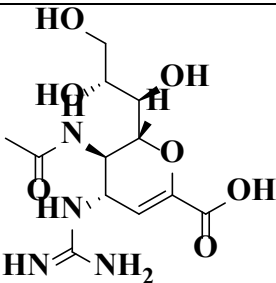
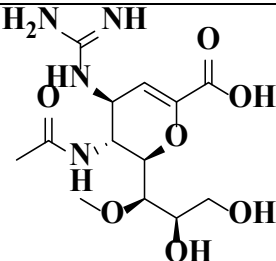
Molecular Docking Results Analysis

Twenty-one compounds obtained from the pharmacophore filtering step proceeded to molecular docking screening against H7N9 protein of AIV A. The results indicated that five compounds (5, 29, 87, 140, and 214) showed stronger binding affinity than co-crystallized ligand (Table S3 and Figure S1). Compound 5 was found to demonstrate an excellent binding affinity of -57.1741 kcal/mol. The hydroxyl group of benzene rings and carbonyl group were established hydrogen bonds with Glu 278, Glu229 and Arg372 residues respectively. While the hydroxyl oxygen mediated a hydrophobic interaction with Arg226. Two benzene rings also projected two pi-anion bonds with Asp152 and Glu179 residues. The methyl group's hydrogen also mediated four alkyl/pi-alkyl bonds with Arg153, Trp180, Ile224 and Arg226 residues. On the one hand, compound 29 showed the binding affinity of -48.6009 kcal/mol toward the protein. Carbonyl and hydroxyl group from benzene ring projected two hydrogen bonds with Glu120 and Arg153 residues, respectively, and an amine group was also found to form a hydrogen bond with Asn348. Two benzene rings were observed to form pi-cation and alkyl/pi-alkyl bonds with Arg119, Arg319 and Ala248 residues respectively. Methyl group of benzene was also found to interact with Ile224 by an alkyl/pi-alkyl bond.

Compound 87 demonstrated the best binding affinity with the binding affinity value of -52.0339 kcal/mol. Interaction analysis of the binding mode of compound 87 in target protein revealed that it forms seven hydrogen bonds with Arg119, Asp152, Arg153, Ser181, Glu229, Lys294 and Arg372 amino acid residues. Besides, compound 140 was also found to show a strong binding affinity (-54.5009 kcal/mol). Two carbonyl groups projected three hydrogen bonds with the Arg119, Ser181 and Arg372 residues. While the hydroxyl group also showed two hydrogen bonds with Glu278 and Lys294 residues. The halogen Fluorine

projected two hydrogen bonds with Asn348 and Lys434 as well as a hydrophobic interaction with Arg372 residue. Two benzene rings mediated one pi-anion with Glu279 and one pi-alkyl with Pro433 residue. Lastly, compound 214 showed a good binding affinity with the binding energy of -50.8905 kcal/mol. Two carbonyl groups were formed two hydrogen bonds with Arg119 and Arg153 residues respectively. Hydroxyl hydrogen of benzene ring was observed to interact with Glu120 and Asp152 residues by hydrogen bonds. Benzene ring also showed pi-anion and pi-alkyl bonds with Asp152, Glu179 and Ala248 residues respectively.

Table 1. Training Set of Compounds to built a Pharmacophore Model of Avian Influenza A Virus

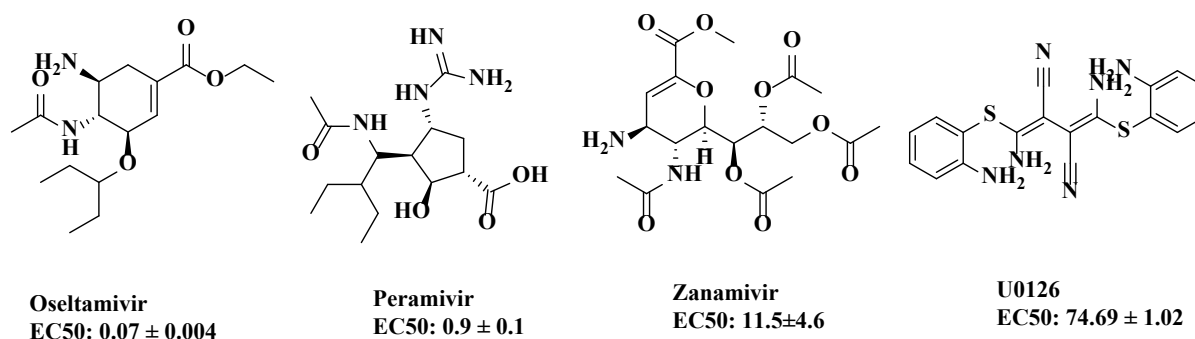
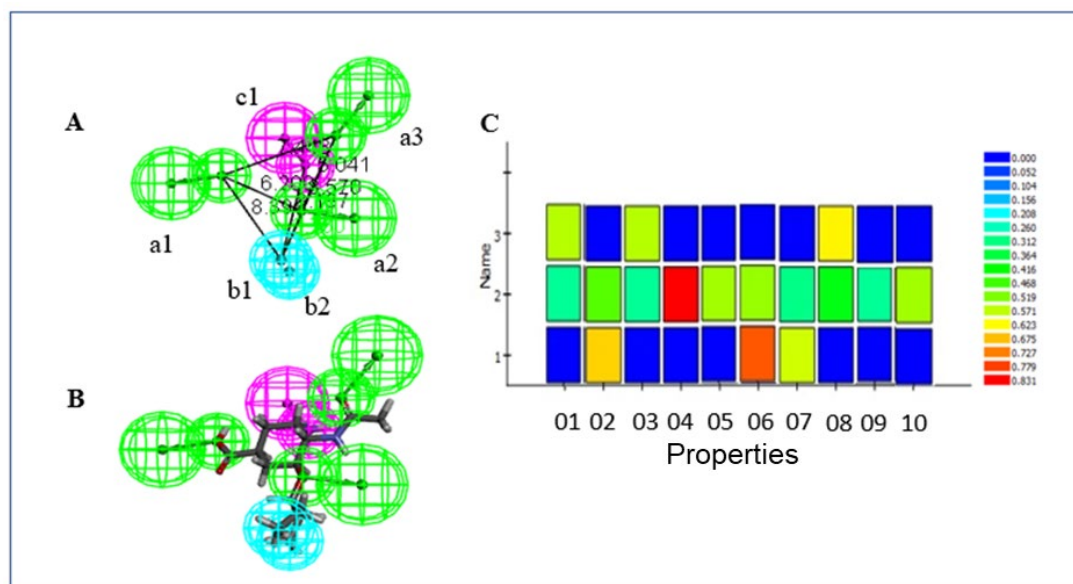
Index Number	Structure	PDB	IC ₅₀ Value	Reference
01		4MWV	0.40 μ M	[19]
02		4MWW	0.79 μ M	[19]
03		4MWX	0.41 μ M	[19]
04		4MWY	3.24 μ M	[19]

Notes: IC₅₀ values were calculated according to the relevant literature.

Table 2. Chemical properties of the ten possibilities derived from four active compounds derived from four Avian Influenza A virus proteins (4MWV, 4MWW, 4MWX and 4MWY)

Hypothesis	Feature	PDB ID	Rank	Max Fit
01	DDDDAAA	4MWY	17.776	7
02	DDDDAAA	4MWY	17.761	7
03	HHDDAA	4MWV	13.824	6
04	HHDDAA	4MWV	13.822	6
05	HHDDAA	4MWV	13.822	6
06	HHDAAA	4MWW	13.364	6
07	HHDAAA	4MWW	13.357	6
08	HHDAAA	4MWW	13.357	6
09	DAAAA	4MWX	12.271	5
10	DAAAA	4MWX	12.271	5

Notes: H denotes the hydrophobic group, D is the hydrogen bond donor, and A denotes the hydrogen bond acceptor. (b) The compound ranking score from the training set that best fits the hypothesis. The greater the rank, the less probable it is that the compounds in the training set have a probable relationship with the hypothesis. The best hypothesis is the most valuable hypothesis.

**Figure 2.** The Test Set (More Active to Less Active) for Pharmacophore Model Validation of Avian Influenza A Virus**Figure 3.** HipHop pharmacophore Generation. The HipHop-Hypo06 (A) The pharmacophore characteristics, HBA and H, are green and blue in hue, respectively. (B) Chemical properties of HipHop-Hypo06. (C) A heat map of the test's ten hypotheses

Docking Validation

To confirm the docking approach, the co-crystallized ligand of the target protein was re-docked into the corresponding binding areas of Avian-origin Human-infecting H7N9 Influenza (PDB ID: 4MWW; Resolution: 1.90) (Figure S1). The co-crystallized ligand interacted to the target protein with the binding energy of -48.2195 kcal/mol with the four hydrogen bonds. The co-carbonyl group of co-crystallized ligand formed a hydrogen link with the Arg372 residue, while the hydroxyl group formed two hydrogen bonds with the Arg119 and Glu120 residues. Furthermore, the hydrogen of the amine group formed a hydrogen connection with the Glu278 residue. The hydrogen of the benzene ring interacted hydrophobically with the Glu279 residue. Furthermore, the methyl group formed two alkyl bonds with the amino acid residues Ile224 and Arg226. Figure 4.37 depicts the docking contacts between the co-crystallized ligand and the target protein.

According to Wu et al., (2013), Shanghai N9 has a Ile294, which forms a salt bridge with Glu276, causing Glu276 to adopt a conformation that prevents the oseltamivir pentyloxy group from binding. Glu276 exhibits the same conformations as in the uncomplexed Shanghai N9-oseltamivir carboxylate complex structure. The oseltamivir carboxylate pentyloxy group is pushed away from the active site by this unfavourable interaction. On the other hand, Ile294 is too far away (by 2.98 Å) from Glu276, which is orientated toward Ile224, a conformation that favours oseltamivir carboxylate binding [19].

ADMET Prediction

Based on the ADMET prediction findings evaluated with a value of 150, all compounds were determined to be effectively digested in the human intestine. Compounds 5 and 214, in particular, with the vanillin moiety, demonstrated a potential logarithm of molar solubility value range of -5.391 and -5.281, respectively. These compounds are also water soluble, whereas the others are not. Compound 5 was expected to have a plasma protein binding of $\geq 90\%$, while the other compounds had a plasma protein binding of $\leq 90\%$. All of the medications were found to have a high Blood-Brain Barrier (BBB) permeability as well as a high hepatotoxicity profile. The information is summarised in Table 3.

Drug-likeness

Among the five compounds (5, 29, 87, 140, and 214), four exhibited a fair chance of excellent absorption with logP values ranging from 3.63 to 5.07. Compounds 5, 84, and 214 were discovered to have TPSA values ranging from 110.14 to 136.17. All of the compounds have a lower range of rotatable bonds than 10. As a result, they have little conformational flexibility. Furthermore, compounds 5 and 214 have low molecular weights of 400.43 and 507.52, respectively, due to having seven and nine hydrogen bond acceptors (nON) that are less than 10 and four and two hydrogen bond donors (nONH) that are less than 5. Finally, compounds 5 and 214 contain 29 and 36 atoms, which are

Table 3. ADMET Prediction of Best Compounds for Avian Influenza A Virus

Compound Number	Human Intestinal Absorption			Aqueous Solubility		Blood Brain Barrier (BBB) Penetration		Plasma Protein Binding (PPB)	Hepatotoxicity
	PSA ^a	ALogP98 ^b	Level ^c	Log (Sw) ^d	Level ^e	LogBB ^f	Level ^g	Prediction ^h	Prediction ⁱ
5	130.41	5.01	2	-5.39	2	0	4	1	1
29	141.37	4.85	2	-6.89	1	0	4	0	1
87	111.39	4.82	2	-7.90	1	0	4	0	1
140	144.09	4.16	2	-7.10	1	0	4	0	1
214	135.20	3.43	2	-5.28	2	0	4	0	1
Co-crystallized ligand	103.69	0.31	0	-1.52	4	1.698	3	0	0

^a Polar surface area (PSA) (>150 : extremely low absorption).

^b Log P based Atom (ALog P98) (≤ 2.0 or $P \geq 0$: extremely low absorption).

^c Prediction of human intestine absorption level; 0 (excellent), 1 (moderate), 2 (poor), 3 (very poor).

^d The log(Sw) based 10 logarithm of molar solubility (25°C, pH = 7.0) (acceptable drug-like compounds: $6 < \log(\text{Sw}) \leq 0$).

^e Prediction of aqueous solubility level: 0 (extremely low), 1 (very low), 2 (low), 3 (good), 4 (optimal), 5 (too soluble), 6 (warning: molecules with one or more unknown Alog P calculation).

^f Extremely strong penetrants (log BBP ≥ 7).

^g Prediction of blood brain barrier penetration level: 0 (very high penetrate), 1 (high), 2 (medium), 3 (low), 4 (undefined).

^h Predicting Plasma-protein binding (0: $<90\%$; $1 \geq 90\%$).

ⁱ Prognosis of hepatotoxicity (0: non-toxic; 1: toxic).

Table 4. Drug-likeness Properties of Best Compounds for Avian Influenza A Virus

Compound Number	MiLogP	TPSA	n. A.	MW	n ON	N ONH	n. V.	n. R.	Vol
5	5.07	128.19	29	400.43	7	4	1	6	357.14
29	4.52	141.34	37	582.43	9	4	1	5	437.31
87	6.04	110.14	42	624.36	7	2	2	8	438.57
140	4.02	141.36	41	586.44	8	4	1	7	449.02
214	3.63	136.17	36	507.52	9	2	1	6	418.64
Co-crystallized ligand	-0.14	101.65	20	284.36	6	4	0	6	275.27

Millog P: partition coefficient ≤ 5

TPSA: Topological polar surface area $\geq 140 \text{ \AA}^2$

n A: number of atoms 20 - 70

MW: molecular weight ≤ 500

n ON: number of hydrogens acceptor ≤ 10

nONH: number of hydrogen donor ≤ 5

nV: number of violations of five Lipinsky rules.

n.R: number of rotatable bonds and vol volume of molecule > 10

both within the range of 20-70. According to the data from Table 4, compounds 5 and 214 followed the Lipinski's rule of five.

CYP Inhibitor Analysis

There are many CYP enzyme isoforms that play important roles in drug metabolism, including CYP3A4, CYP2D6, CYP2C9, CYP2C19, and CYP1A2. The first and most significant isoform is CYP3A4 [16], which is responsible for 50% of the drug's metabolism in the intestine and kidney. It is crucial to ascertain whether the pharmaceutical candidate in question is capable of inhibiting a certain CYP enzyme isoform. It is assumed that drugs that do not become antagonists of all CYP isoforms are safe [31]. Inhibitors may impair an enzyme's metabolic capacity. As a result, compound 5 has a negative value for the CYP1A2, CYP2C19, and CYP2D6 isoforms. Table 5 summarises the

information.

Bulky moieties such as prenyl and geranyl, according to Park et al., (2011) and Moradi et al., (2011), play an important role in antiviral action against the Influenza A virus [32,33]. It is also suggested that compound 5 may be effective against Avian Influenza A.

Finally, the lead compound 5 (Figure 4) was well-mapped into the produced pharmacophore, with a best fit value of 3.34017. Compound 5, on the other hand, demonstrated a strong binding affinity to the Avian-origin Human-infecting H7N9 Influenza, with a binding energy of -57.1741 kcal/mol. Compound 5 formed three hydrogen bonds with the residues Glu278, Glu229, and Arg372, as well as one hydrophobic contact with the residue Arg226. The lead drug-likeness and ADMET properties were both acceptable of compound 5. Compound 5, on the other hand, has been discovered to have a negative value for the CYP1A2, CYP2C19, and CYP2D6 isoforms.

Table 5. CYP Inhibitor of Best Compound for Avian Influenza A Virus

Compound Number	CYP1A2 inhibitor	CYP2C19 inhibitor	CYP2C9 inhibitor	CYP2D6 inhibitor	CYP3A4 inhibitor	Log K_p (skin permeation)
5	No	No	Yes	No	Yes	-4.83 cm/s
214	No	Yes	Yes	No	Yes	-6.34 cm/s
Co-crystallized ligand	No	No	No	No	No	-9.36 cm/s

No= non-inhibitor; Yes= inhibitor

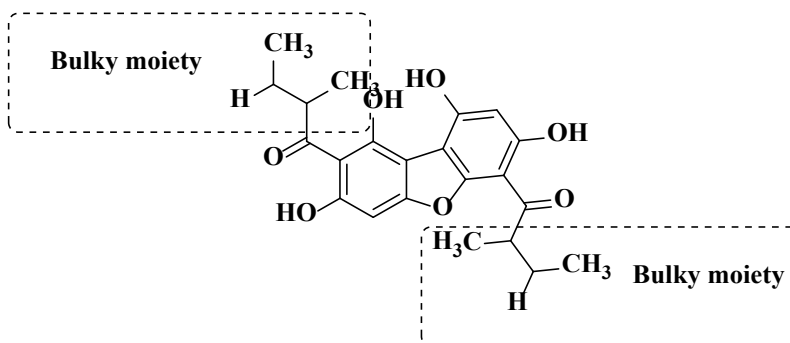


Figure 4. Lead Compound as anti-AIV A Virus (Compound 5)

CONCLUSION

New and improved antiviral therapies are required to combat the Human Affecting Avian Influenza A (H7N9) virus. The researchers sought to see if a chemical present in Usnic acid derivatives may fight AIV A. (H7N9). A total of 340 usnic acid derivatives were tested for pharmacophore mapping, with the top 21 compounds selected based on the greatest suit value (>3.30). The twenty-one compounds were then molecular docked, with the results indicating five compounds (Compounds 5, 29, 87, 140, and 214) that were consistent with the active region of the avian influenza H7N9 protein. To study the pharmacokinetics and drug scan characteristics, these compounds were submitted to ADMET prediction and drug-likeness properties. The selected two compounds are next subjected to CYP isoform analysis in order to identify the lead compound 5. Overall, we conclude that compound 5 should be investigated further and perhaps developed as a strong anti-AIV A agent.

ACKNOWLEDGEMENTS

The authors would like to thank the Ministry of Higher Education for providing financial support under the Fundamental Research Grant Scheme (FRGS) No. FRGS/1/2018/TK05/UTM/02/18 (University Reference RDU1901160) and Universiti Malaysia Pahang for laboratory facilities as well as additional financial support under Internal Research Grant RDU1803148. The authors also would like to thank the Faculty of Pharmacy, Universiti Kebangsaan Malaysia (UKM) for providing Discovery Studio 3.1 software.

REFERENCES

- Eweas, A. F., and Abdel-Moneim, A. S. (2015) In-silico structural analysis of the influenza A subtype H7N9 neuraminidase and molecular docking with different neuraminidase inhibitors. *Virusdisease*, 26(1), 27-32.
- Hasan, M., Ghosh, P. P., Azim, K. F., Mukta, S., Abir, R. A., Nahar, J., and Khan, M. M. H. (2019) Reverse vaccinology approach to design a novel multi-epitope subunit vaccine against avian influenza A (H7N9) virus. *Microbial pathogenesis*, 130, 19-37.
- Chen, Y., Liang, W., Yang, S., Wu, N., Gao, H., Sheng, J., and Yuen, K. Y. (2013) Human infections with the emerging avian influenza A H7N9 virus from wet market poultry: clinical analysis and characterisation of viral genome. *The Lancet*, 381(9881), 1916-1925.
- Seniya, C., Khan, G. J., Misra, R., Vyas, V., and Kaushik, S. (2014) In-silico modelling and identification of a possible inhibitor of H1N1 virus. *Asian Pacific Journal of Tropical Disease*, 4, S467-S476.
- Russell, R. J., Haire, L. F., Stevens, D. J., Collins, P. J., Lin, Y. P., Blackburn, G. M., and Skehel, J. J. (2006) The structure of H5N1 avian influenza neuraminidase suggests new opportunities for drug design. *Nature*, 443(7107), 45-49.
- Yi Tsang, N., Zhao, L. H., Wai Tsang, S., and Zhang, H. J. (2017) Antiviral Activity and Molecular Targets of Plant Natural Products Against Avian Influenza Virus. *Current Organic Chemistry*, 21(18), 1777-1804.
- WHO (2007). Cumulative Number of Confirmed Human Cases of Avian Influenza A/(H5N1) Reported to WHO, accessed at http://www.who.int/csr/disease/avian_influenza/country/cases_table_2007_06_29/en/index.html
- Kuo, H. I., Chang, C. L., Huang, B. W., Chen, C. C., and McAleer, M. (2009) Estimating the impact of avian flu on international tourism demand using panel data. *Tourism Economics*, 15(3), 501-511.
- World Health Organization. Influenza at the human-animal interface http://www.who.int/influenza/human_animal_interface/Influenza_Summary_IRA_HA_interface_27June14.pdf?ua=1 (Accessed Jan 20, 2016).
- Centre for Health Protection. Avian Influenza Report http://www.chp.gov.hk/files/pdf/2014_avian_influenza_report_vol10_wk34.pdf (Accessed Jan 22, 2016).
- Hsieh, H. P., and Hsu, J. T. A. (2007) Strategies of development of antiviral agents directed against influenza virus replication. *Current pharmaceutical design*, 13(34), 3531-3542.
- Wang, S. Q., Du, Q. S., Huang, R. B., Zhang, D. W., and Chou, K. C. (2009) Insights from investigating the interaction of oseltamivir (Tamiflu) with neuraminidase of the 2009 H1N1 swine flu virus. *Biochemical and Biophysical Research Communications*, 386(3), 432-436.
- Blumenkrantz, D., Roberts, K. L., Shelton, H., Lycett, S., and Barclay, W. S. (2013) The short stalk length of highly pathogenic avian

- influenza H5N1 virus neuraminidase limits transmission of pandemic H1N1 virus in ferrets. *Journal of virology*, 87(19), 10539-10551.
14. Wu, Y., Wu, Y., Tefsen, B., Shi, Y., and Gao, G. F. (2014) Bat-derived influenza-like viruses H17N10 and H18N11. *Trends in microbiology*, 22(4), 183-191.
15. Capua, I., and Marangon, S. (2006) Control of avian influenza in poultry. *Emerging Infectious Diseases*, 12(9), 1319-1324.
16. An, J., Lee, D. C., Law, A. H., Yang, C. L., Poon, L. L., Lau, A. S., and Jones, S. J. (2009) A novel small-molecule inhibitor of the avian influenza H5N1 virus determined through computational screening against the neuraminidase. *Journal of medicinal chemistry*, 52(9), 2667-2672.
17. Sokolov, D. N., Zarubaev, V. V., Shtro, A. A., Polovinka, M. P., Luzina, O. A., Komarova, N. I., and Kiselev, O. I. (2012) Anti-viral activity of (-)- and (+)-usnic acids and their derivatives against influenza virus A (H1N1) 2009. *Bioorganic and medicinal chemistry letters*, 22(23), 7060-7064.
18. Ingolfssdottir, K. (2002) Usnic acid. *Phytochemistry*, 61(7), 729-736.
19. Wu, Y., Bi, Y., Vavricka, C. J., Sun, X., Zhang, Y., Gao, F., and Gao, G. F. (2013) Characterization of two distinct neuraminidases from avian-origin human-infecting H7N9 influenza viruses. *Cell research*, 23(12), 1347-1355.
20. Thangapandian, S., John, S., Sakkiath, S., and Lee, K. W. (2011) Molecular docking and pharmacophore filtering in the discovery of dual-inhibitors for human leukotriene A4 hydrolase and leukotriene C4 synthase. *Journal of chemical information and modeling*, 51(1), 33-44.
21. Liu, C., Yin, J., Yao, J., Xu, Z., Tao, Y., and Zhang, H. (2020) Pharmacophore-based virtual screening toward the discovery of novel anti-echinococcal compounds. *Frontiers in cellular and infection microbiology*, 10, 1-12.
22. Balaramnavar, V. M., Ahmad, K., Saeed, M., Ahmad, I., Kamal, M., and Jawed, T. (2020) Pharmacophore-based approaches in the rational repurposing technique for FDA approved drugs targeting SARS-CoV-2 Mpro. *RSC Advances*, 10(66), 40264-40275.
23. Chen, J., Jiang, H., Li, F., Hu, B., Wang, Y., Wang, M., and Cheng, M. (2018) Computational insight into dengue virus NS2B-NS3 protease inhibition: A combined ligand- and structure-based approach. *Computational biology and chemistry*, 77, 261-271.
24. Aluwi, M. F. F. M., Rullah, K., Haque, M. A., Yamin, B. M., Ahmad, W., Amjad, M. W., and Lam, K. W. (2017) Suppression of PGE 2 production via disruption of MAPK phosphorylation by unsymmetrical dicarbonyl curcumin derivatives. *Medicinal Chemistry Research*, 26(12), 3323-3335.
25. Roney, M., Moyeenul Huq, A. K. M., Rullah, K., Hamid, H. A., Imran, S., Islam, M. A., and Mohd Aluwi, M. F. F. (2021) Virtual Screening-based Identification of Potent DENV-3 RdRp Protease Inhibitors via in-house Usnic Acid Derivatives Database. *Journal of Computational Biophysics and Chemistry*, 20(6), 1-18.
26. Razzaghi-Asl, N., Mirzayi, S., Mahnam, K., and Sepehri, S. (2018) Identification of COX-2 inhibitors via structure-based virtual screening and molecular dynamics simulation. *Journal of Molecular Graphics and Modelling*, 83, 138-152.
27. Ibrahim, M. K., Eissa, I. H., Alesawy, M. S., Metwaly, A. M., Radwan, M. M., and ElSohly, M. A. (2017) Design, synthesis, molecular modeling and anti-hyperglycemic evaluation of quinazolin-4 (3H)-one derivatives as potential PPAR γ and SUR agonists. *Bioorganic and medicinal chemistry*, 25(17), 4723-4744.
28. El-Zahabi, M. A., Elbendary, E. R., Bamanie, F. H., Radwan, M. F., Ghareib, S. A., and Eissa, I. H. (2019) Design, synthesis, molecular modeling and anti-hyperglycemic evaluation of phthalimide-sulfonylurea hybrids as PPAR γ and SUR agonists. *Bioorganic chemistry*, 91, 1-17.
29. Mishra, S. S., Sharma, C. S., Singh, H. P., Pandiya, H., and Kumar, N. (2016) *In-silico* ADME, Bioactivity and toxicity parameters calculation of some selected anti-tubercular drugs. *International Journal of Pharmacological and Phytopharmacological Research*, 6, 77-79.
30. Daina, A., Michielin, O., and Zoete, V. (2017) SwissADME: a free web tool to evaluate pharmacokinetics, drug-likeness and medicinal chemistry friendliness of small molecules. *Scientific reports*, 7(1), 1-13.
31. Bagastama, A. R., Alkaff, A. H., and Tambunan, U. S. F. (2020) Discovery of Natural Product Compounds as Dengue Virus NS5 Methyltransferase Inhibitor Candidate through *in-silico* Method. In *Key Engineering Materials*, 840, 270-276.
32. Park, J. Y., Jeong, H. J., Kim, Y. M., Park, S. J., Rho, M. C., Park, K. H., and Lee, W. S. (2011) Characteristic of alkylated chalcones from *Angelica keiskei* on influenza virus neuraminidase inhibition. *Bioorganic and medicinal chemistry letters*, 21(18), 5602-5604.
33. Moradi, M. T., Karimi, A., and Lorigooini, Z. (2018) Alkaloids as the natural anti-influenza virus agents: a systematic review. *Toxin Reviews*, 37(1), 11-18.